SYNTHESIS, STRUCTURE, AND ANTIMICROBIAL ACTIVITY OF COMPLEXES OF BIVALENT METALS WITH 1-NAPHTHYLACETIC ACID **

L. A. Albedair

Department of Chemistry, College of Science at Princess Nourah Bint Abdulrahman University, Riyadh 11671, Saudi Arabia; e-mail: lamiaalbedair@gmail.com

*1-Naphthylacetic acid ($C_{10}H_7$-CH_2COOH; HL) is a synthetic commercial plant hormone widely used in agriculture as a plant growth regulator. Five complexes between metal and this hormone were synthesized and structurally characterized: $[MnL_2(H_2O)_2]$ (**A**), $[CoL_2(H_2O)_2]$ (**B**), $[NiL_2]$ (**C**), $[CuL_2(H_2O)_2]$ (**D**), and $[ZnL_2] \cdot H_2O$ (**E**). Next, IR, ^{1}H NMR, UV-Vis, thermogravimetry, magnetic moment, and elemental analyses were used to characterize the complexes, and their morphological properties were assessed using XRD and SEM techniques. These analyses indicated that two L^- molecules were coordinated to the metal ion by their bidentate carboxylate groups. Finally, the complexes were screened in vitro against several microbes (bacteria and fungi) using the Kirby–Bauer disc diffusion method. Complex **C** showed antifungal activity against Candida albicans with a potency that was 15% higher than the antifungal drug amphotericin B.*

Keywords: *1-naphthylacetic acid, spectroscopy, carboxylate group, antimicrobial activity.*

СИНТЕЗ, СТРОЕНИЕ И АНТИМИКРОБНАЯ АКТИВНОСТЬ КОМПЛЕКСОВ ДВУХВАЛЕНТНЫХ МЕТАЛЛОВ С 1-НАФТИЛУКСУСНОЙ КИСЛОТОЙ

L. A. Albedair

УДК 543.42

Научный колледж при Университете принцессы Нуры Бинт Абдулрахман, Эр-Рияд 11671, Саудовская Аравия; e-mail: lamiaalbedair@gmail.com

(Поступила 2 июля 2020)

*Синтезированы и структурно охарактеризованы пять комплексов металлов и синтетического гормона роста растений 1-нафтилуксусной кислоты ($C_{10}H_7$-CH_2COOH; HL): $[MnL_2(H_2O)_2]$ (**A**), $[CoL_2(H_2O)_2]$ (**B**), $[NiL_2]$ (**C**), $[CuL_2(H_2O)_2]$ (**D**) и $[ZnL_2] \cdot H_2O$ (**E**). Для характеристики комплексов использованы ИК-, ^{1}H ЯМР-, УФ-видимая спектроскопия, термогравиметрия, магнитно-резонансный и элементный анализ. Морфологические свойства оценены с помощью методов рентгенографии и сканирующей электронной спектроскопии. Показано, что две L^- молекулы скоординированы с ионом металла их бидентатными карбоксилатными группами. Комплексы подвергались скринингу in vitro против нескольких микробов (бактерий и грибков) с использованием метода дисковой диффузии Кирби–Бауэра. Комплекс **C** проявлял противогрибковую активность против Candida albicans с эффективностью на 15 % выше, чем противогрибковый препарат амфотерицин B.*

Ключевые слова: *1-нафтилуксусная кислота, спектроскопия, карбоксилатная группа, антимикробная активность.*

Introduction. Agrochemicals such as plant-growth regulators, pesticides, herbicides, and fertilizers are essential for modern agriculture. Plant growth regulators are endocrine-disrupting compounds. These compounds integrate extracellular signals to enhance agricultural characteristics, improve production, and modulate plant growth [1–3]. Auxins are a group of small-molecule plant hormones generated by plant cells that are involved in a wide variety of biological processes in plants and have attracted considerable interest due to their physiological and biological impact [4–6].

**Full text is published in JAS V. 88, No. 6 (http://springer.com/journal/10812) and in electronic version of ZhPS V. 88, No. 6 (http://www.elibrary.ru/title_about.asp?id=7318; sales@elibrary.ru).

1-Naphthylacetic acid ($C_{10}H_7$-CH_2COOH) is an aromatic acid that takes the form of a white solid powder with a molecular weight of 186.2 g and a melting point of 135°C; it is soluble in organic solvents. This naphthalene derivative belongs to the synthetic branch of auxins and features a carboxymethyl group (CH_2CO_2H) linked to position "1" of naphthalene. Among the auxins, this one is widely used in the world of farming as a plant growth regulator in agriculture. It regulates a number of plant development functions. Examples of these functions include i) controlling flower induction, ii) preventing pre-harvest fruits from dropping (e.g., grapes, plums, grapefruits, oranges, nectarines, peaches, tomatoes, strawberries, pears, mangos, and pineapples), iii) fruit-thinning (e.g., olives, potatoes, apples, and citrus fruits), and iv) promoting seed germination [7]. Aromatic acids are very important in biochemical and biological processes: 1-naphthylacetic acid is an aromatic acid with structural stability via the rigid isoelectronic structure of naphthalene and a large conjugated plane [8].

Transition metals form complexes with carboxylate anions. A versatile carboxylate anion can adopt a wide range of bonding modes including monodentate, symmetric and asymmetric chelating, and bidentate and monodentate bridging [9]. It is generally known that the carboxylate complexes of the 3*d* elements including several examples of nickel, cobalt, manganese, copper, and zinc derivatives play an important role in biochemistry [10]. Of these, salicylic acid, its derivatives, as well as some copper complexes, have attracted considerable interest from structural and biological viewpoints [11]. Metal complexation can change biological activity of the macromolecules, and new properties can be utilized in many cases in pharmaceutical practice [12]. Transition metal complexes have attracted great interest for their application in industrial and synthetic processes such as catalysis, photochemistry, and biological applications [12].

Complexes of transition metals (Co, Mn, Ni, Zn, and Cu) play an important role in the life processes of living organisms. They are, among others, components of enzymes, proteins, and vitamins; they participate in oxidation–reduction processes or in binding, storage, and transport of oxygen [13, 14]. Here, we describe the synthesis, characterization, and biological activity of transition metal (*d*-block) of 1-naphthylacetic acid (HL) in order to study their biological applications *in vitro*. WE then investigate the spectroscopic behavior and structure of these complexes.

The complexes were screened *in vitro* for their antifungal and antibacterial properties using the Kirby–Bauer disc diffusion method with two fungal and four bacterial microbes [15–17].

Experimental. *Chemicals and instrumentation.* All preparations and experiments were performed using analytical grade chemicals, Milli-Q purified water (Milli-Q system, Millipore, Bedford, MA, USA), and pure solvents; all were used as received without further purification. The 1-naphthylacetic acid ($C_{12}H_{10}O_2$; 186.2 g/mol; purity ≥95.0%) was obtained from Fluka (Seelze, Germany). The chloride salts $MnCl_2·4H_2O$, $CoCl_2·6H_2O$, $NiCl_2·6H_2O$, $CuCl_2·H_2O$, and $ZnCl_2$ had a of purity 98–99.5% and were from Sigma-Aldrich Company (St. Louis, MO, USA). Analytical measurements were acquired using a PE 2400CHN elemental analyzer for microanalyses and a Sherwood magnetic susceptibility balance for the mass susceptibilities (X_g). The spectral measurements were conducted at room temperature using a Bruker FT-IR spectrophotometer for IR spectra (KBr discs), a Bruker DRX-250 spectrometer for ^{1}H NMR spectra (DMSO-d_6 solution, 600 MHz), a UV2-Unicam UV/Vis spectrophotometer for UV-Vis spectra (DMSO solvent), and X'Pert Philips X-ray diffractometer for XRD spectra (2θ 5–80°; Cu$K_{\alpha1}$; λ = 0.154056 nm). Thermal measurements were conducted using a Shimadzu TGA-50H thermal analyzer (25–800°C, nitrogen atmosphere). Structural morphologies were visualized using a Quanta FEG 250 scanning electron microscope (10 kV accelerating voltage).

Preparations. One millimole of each metal chloride, $MnCl_2·4H_2O$, $CoCl_2·6H_2O$, $NiCl_2·6H_2O$, $CuCl_2·H_2O$, and $ZnCl_2$ were dissolved in Milli-Q purified water (25 mL) and then mixed separately with 2.0 mmol HL in methanol (25 mL). Ammonium solution (5%) was added to adjust the pH to 7. The resulting mixtures were kept at 60°C for 20 min under intense stirring. After cooling, the colored precipitates were isolated, filtered, thoroughly washed, dried in an oven at 65°C, and then stored at room temperature in a desiccator over anhydrous $CaCl_2$. The Mn(II) ions formed a brown-colored powder, Co(II) ions formed a crimson red-colored powder, Ni(II) ions formed an oily green-colored powder, Cu(II) ions formed a greenish blue-colored powder, and Zn(II) ions formed a yellowish white-colored powder. The complexes are formulated as $[MnL_2(H_2O)_2]$ (**A**), $[CoL_2(H_2O)_2]$ (**B**), $[NiL_2]$ (**C**), $[CuL_2(H_2O)_2]$ (**D**), and $[ZnL_2]H_2O$ (**E**), respectively. Complexes **A**, **B**, **C**, **D**, and **E** were characterized by spectral, thermal, and elemental analyses.

Antimicrobial assays. The complexes were assayed *in vitro* for their antifungal and antibacterial properties against two fungi and four bacteria using the Kirby–Bauer disc diffusion method [15–17]. The bacterial species were two Gram-negative strains (*E. coli* and *P. aeruginosa*) and two Gram-positive strains (*S. aureus*

and *B. subtilis*); the fungal species were *A. flavus* and *C. albicans*. The type of strain of microorganisms can be mentioned as follows:

Name	Gram reaction	ATCC
Bacillus subtilis	G^+	6051
Escherichia coli	G^-	11775
Pseudomonas aeruginosa	G^-	10145
Staphylococcus aureus	G^+	12600
Candida albicans	Fungus	7102
Aspergillus flavus	Fungus	9643

The antimicrobial results of the complexes were compared with those of the free HL ligand and the antibiotic drugs (tetracycline for antibacterial and amphotericin B for antifungal assays).

Results and discussion. *Elemental analysis.* Mn(II), Co(II), Ni(II), Cu(II), and Zn(II) chlorides were dissolved in Milli-Q purified water where the ligand was dissolved in methanol solvent. The colored precipitates were collected for each reaction at pH 7, which were insoluble in most organic solvents and water except dimethyl sulfoxide (DMSO) and N,N-dimethylformamide-based solvents. In each complex, the percentage (%) of carbon and hydrogen was determined using CHN elemental analysis where the metal element was determined gravimetrically. The reaction stoichiometry for all complexes was 1:2 (metal:ligand) suggesting that the complexes were formulated as $[MnL_2(H_2O)_2]$ (**A**), $[CoL_2(H_2O)_2]$ (**B**), $[NiL_2]$ (**C**), $[CuL_2(H_2O)_2]$ (**D**), and $[ZnL_2]H_2O$ (**E**):

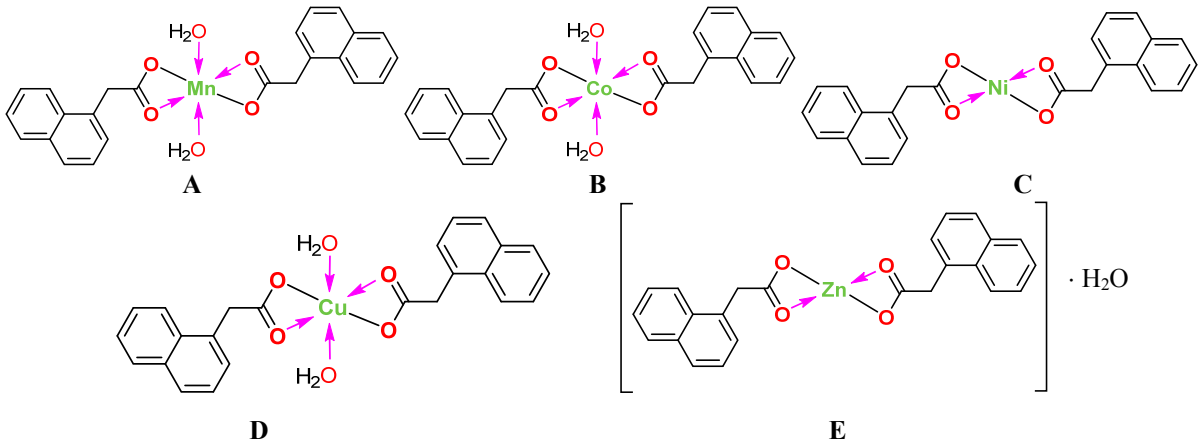

The corresponding elemental analyses are (**A**) Anal. Found: C, 62.28; H, 4.90; M, 11.72%, Calcd: C, 62.43; H, 4.77; M, 11.91%, (**B**) Anal. Found: C, 62.07; H, 4.88; M, 12.44%, Calcd: C, 61.89; H, 4.73; M, 12.66%, (**C**) Anal. Found: C, 62.26; H, 4.08; M, 13.52%, Calcd: C, 67.12; H, 4.19; M, 13.68%, (**D**) Anal. Found: C, 61.43; H, 4.54; M, 13.48%, Calcd: C, 61.28; H, 4.68; M, 13.52%, and (**E**) Anal. Found: C, 63.25; H, 4.59; M, 14.22%, Calcd: C, 63.46; H, 4.41; M, 114.41%.

Table 1 lists the thermal decomposition data of the synthesized complexes obtained from the thermograms. The thermal decomposition data of the complexes enabled the following observations:

1. Complex **D** exhibited good thermal stability up to 250°C. Complex **E** lost the lattice water molecule at around 80°C, but the complex remained thermally stable until 300°C. Complexes **A**, **B**, and **C** started their thermal decompositions at around 100°C.

2. Complexes **A**, **B**, and **E** exhibited a three-stage degradation process while complexes **C** and **D** degraded in two stages.

3. The release and pyrolysis of the first L^- molecule began and ended in the first degradation step for complexes **C** and **D** and in the second degradation step for complexes **A**, **B**, and **E**.

4. For all complexes, the pyrolysis of the second L^- molecule began after 400°C.

5. The final decomposition residues of the complexes were metal oxides. For complexes **A**, **B**, and **D**, it was MnO, CoO, and CuO, respectively, contaminated with some residual carbons. Complexes **C** and **E** were NiO and ZnO, respectively, free of any residual carbons.

TABLE 1. Thermal Decomposition of the Synthesized Complexes

Complex	Stages	TG range, °C	TG% mass loss		Lost species
			Found	Calculated	
A	I	110–200	8.06	7.80	$2H_2O$
	II	200–340	40.89	40.14	L^-
	III	340–600	31.15	31.43	$C_{10}H_9O$
	Residue	–	19.35	20.58	MnO + 2C
B	I	115–168	8.04	7.74	$2H_2O$
	II	168–410	39.25	39.80	L^-
	III	410–650	30.92	31.16	$C_{10}H_9O$
	Residue	–	21.30	21.26	CoO + 2C
C	I	100–425	44.48	43.16	L^-
	II	425–730	38.03	39.39	$C_{12}H_9O$
	Residue	–	16.95	17.41	NiO
D	I	250–370	46.52	47.07	$2H_2O + L^-$
	II	370–750	33.90	33.41	$C_{11}H_9O$
	Residue	–	19.51	19.48	CuO + C
E	I	80–140	3.70	3.97	H_2O
	II	140–460	40.19	40.81	L^-
	III	460–700	37.46	37.24	$C_{12}H_9O$
	Residue	–	18.00	17.93	ZnO

FT-IR spectra. Table 2 lists the characteristic IR bands for HL and its metal complexes obtained from their IR spectra. These are illustrated in Fig. 1. Here we discuss the main vibrational assignments. The band characteristic of the acidic OH of HL is absent in the IR spectra of the synthesized complexes. Instead, broad absorption bands appeared in the range of 3590–3350 cm^{-1} characteristic of the OH group ν(O-H) of water suggesting the existence of coordinated or latticed water molecules [18–20]. The C=O group is a multiple bonded group with high polarity, which gives rise to an intense IR absorption band. The stretching vibrations of this group are expected in the 1660–1740 cm^{-1} region [21]. This absorption pattern was observed as a very strong band at 1661 cm^{-1} in the IR spectrum of HL. This characteristic band was not observed in the IR spectra of the synthesized complexes. Rather, two new bands were located around 1559–1541 cm^{-1} due to the $\nu_{as}(COO^-)$ vibrations, and around 1464–1424 cm^{-1} due to the $\nu_s(COO^-)$ vibrations. The carboxylate group (COO^-) coordination to metal ions can be distinguished based on two spectroscopic criteria [22, 23]: the differences between the $\nu_{as}(COO^-)$ and $\nu_s(COO^-)$ values [$\Delta\nu = \nu_{as} - \nu_s$] of the complex compared to the νas(COO^-) vibrations, and around 1464–1424 cm^{-1} due to the νs(COO–) vibrations.

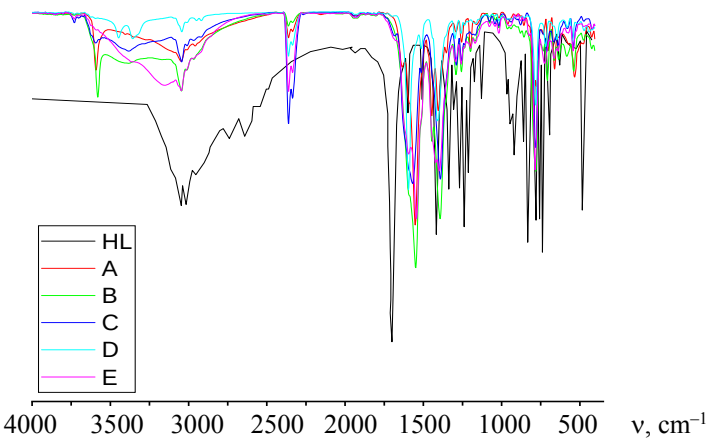

Fig. 1. IR spectra of the HL and its synthesized complexes.

The carboxylate group (COO-) coordination to metal ions can be distinguished based on two spectroscopic criteria [22, 23]: the differences between the $\nu_{as}(COO^{-})$ and $\nu_{s}(COO^{-})$ values [$\Delta\nu = \nu_{as} - \nu_{s}$] of the complex compared to the free ligand anion, and the direction of the $\nu_{as}(COO^{-})$ and $\nu_{s}(COO^{-})$ frequency shifts in the complex compared to that of the free ligand anion. By checking the frequencies of $\nu_{as}(COO^{-})$ and $\nu_{s}(COO^{-})$ and the $\Delta\nu$ values for the synthesized complexes, we found that all of the $\Delta\nu$ values were lower than those of NaL. The $\nu_{as}(COO^{-})$ were shifted toward lower frequencies, and the $\nu_{s}(COO^{-})$ shifted toward higher frequencies indicative of symmetrical bidentate binding of the COO^{-} moiety around the metal atoms. In the IR spectra of the synthesized complexes, the weak bands observed at 421, 425, 426, 436, and 424 cm^{-1} may due to the stretching vibrations of Mn–O, Co-O, Ni-O, Cu–O, and Zn-O bonds, respectively [24].

TABLE 2. Assignments of the IR Spectral Bands (cm^{-1}) for HL and the Synthesized Complexes

HL	**A**	**B**	**C**	**D**	**E**	Assignments
3425	3592	3588	3595, 3380	3450, 3357	3160	ν(O–H)
3073	3050	3048	3047	3042	3048	$\nu_{asym}(CH_2)$
3054	3005	3008	3008	3005	3010	ν_{asym} (CH); ring
2930	2956	2950	2970	2955	2962	ν_{sym}(CH); ring
2912	–	2916	2920	2914	–	$\nu_{sym}(CH_2)$
–	2359	2368	2365	2363	2367	Overtone and combination bands
1693	–	1685	1683	1690	–	δ_{def}(CH); ring
1661	–	–	–	–	–	ν_{sym}(C=O)
1600, 1526	–	–	–	–	–	ν(C=C); ring
–	1552	1550	1553	1559	1541	$\nu_{s}(COO^{-})$
–	1450	1447	1448	1464	1424	$\nu_{as}(COO^{-})$
1410	1402	1392	–	–	–	δ(O-H) in-plane bending
1385	1353	1395	1390	1365	1394	$\delta_{sciss}(CH_2)$
1355, 1327	1288	1292	1294	1294	1294	Ring deformation vibrations
1251	1257	1262	1253	1253	1261	δ_{def}(CH)
1205, 1195	1198	1198	1173	1166	1193	ν(C-C)
1163	1159	1164	1165	1165	1166	$\delta_{rock}(CH_2)$
1135, 1120	–	–	–	–	–	ν(C-O) and δ(C–C)
1073, 1037	1078, 1017	1076, 1017	1079, 1046	1073	1080	Ring breathing vibrations, ν(C–O), and δ(C-C)
1002, 966	957, 857	1010, 958	1012, 939	1012, 952	1019, 945	$\delta_{wag}(CH_2)$
853	870	858	878	866	879	δ(O-H) out-of-plane bending
778, 690	771, 667	778, 662	787, 639	778, 650	785, 664	Ring stretching vibrations
735	730, 707	710, 631	711	718	724	$\delta_{wag}(CH_2)$
538	530	582, 543	560, 543	557, 550	543	$\delta_{twist}(CH_2)$
505, 480, 460	480, 421	475, 425	426	469, 436	473, 424	Ring bending vibrations, ν(M-O)

N o t e: ν, stretching; ν_s, symmetrical stretching; ν_{as}, asymmetrical stretching; δ, bending.

^{1}H NMR spectra. The ^{1}H NMR spectrum of complex **E** (Fig. 2) was collected at room temperature in DMSO-d_6 solvent and compared with HL. The ^{1}H NMR chemical shift for the HL is: δ = 4.03 (s, 2H, CH_2), 7.36 (d, 1H, C2*H*), 7.38 (dd, 1H. C3*H*), 7.46 (dd, 1H. C6*H*), 7.5 (dd, 1H. C7*H*), 7.77 (d, 1H. C5*H*), 7.83 (d, 1H. C4*H*), 7.92 (d, 1H. C8*H*), and 11.00 (s, 1H, COO*H*). The ^{1}H NMR chemical shift for the **E** complex is: δ = 3.89 (s, 2H, CH_2), 7.25 (d, 1H, C2*H*), 7.36 (dd, 1H. C3*H*), 7.39 (dd, 1H. C6*H*), 7.56 (dd, 1H. C7*H*), 7.68 (d, 1H. C5*H*), 7.78 (d, 1H. C4*H*), and 7.99 (d, 1H. C8*H*). The ^{1}H NMR spectrum of HL produced nine signals and all of these proton resonances were observed in the spectrum of complex **E** except that of the COOH group. The characteristic proton of the COOH group in the HL molecule resonated at 11.00 ppm. Its methylene protons resonated at 4.03 ppm. Aromatic protons from the naphthalene ring of HL molecule were observed in the 7.36–7.92 ppm range. Complex **E** had a characteristic signal because the proton of the COOH group in HL was no longer observed. The methylene protons were up-field shifted from 4.03 ppm in

the HL to 3.89 ppm in **E**. Aromatic protons from carbons numbered C2, C3, C4, C5, and C6 shifted up-field; C7 and C8 had down-field shifts in the **E** complex. These shifts in aromatic protons may be due to the electronic effect of the positive metal ion in the complex.

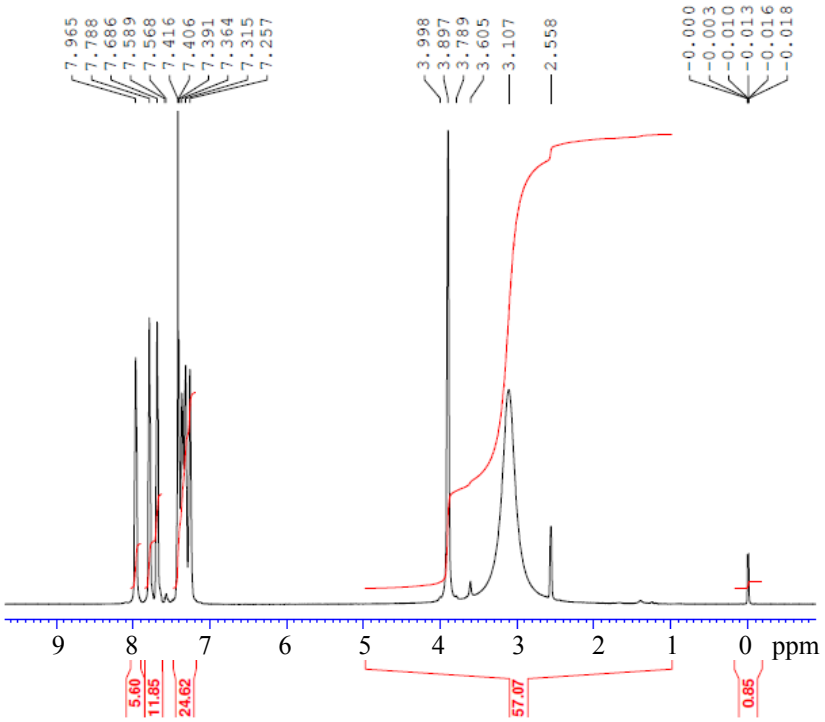

Fig. 2. ^{1}H NMR spectrum of the synthesized zinc(II) complex.

UV–Vis spectra and molar magnetic moment. The HL molecule showed a weak and broad absorption band with a maximum wavelength at (λ_{max} = 281 nm) in its UV-Vis spectrum [25]. This characteristic absorption band of HL was greatly enhanced in its intensity after complexation with the metal ions. We noted a small shift in its wavelength at 284 nm in the spectra of the synthesized complexes. The great increase in the intensity of this band could be due to the $\pi \rightarrow \pi^*$ transitions in the complex. The spectra of the synthesized complexes showed two new bands: The first was in the range of 314–318 nm and corresponded to the $n \rightarrow \pi^*$ transitions; the second one was in the 400–550 nm range, which belongs to the ligand-to-metal charge transfer bands [26]. The molar magnetic moment for the synthesized complexes was determined using the Gouy method [27]. The μ_{eff} values for the synthesized complexes **A**, **B**, **C**, and **D** were 4.5, 4.7, 3.6, and 1.9 B.M., respectively. The values for complexes **A**, **B,** and **D** suggest a paramagnetic property with six-coordinate chelation modes for Cu(II), Co(II), and Mn(II) ions; these complexes have an octahedral structure [28–30]. Complex **B** has a higher μ_{eff} value (4.7 B.M.), indicating that it is likely to have a high spin complex in addition to having an octahedral structure [31]. At room temperature, tetrahedral complexes always exhibit μ_{eff} > 3.3 B.M. (usually in the range of 3.9–3.4 B.M.) The μ_{eff} value of complex **C** falls within in this range (3.6 B.M.), suggesting that the Ni(II) ions assume a four-coordinate chelation mode with tetrahedral stereochemistry. Complex **E** is diamagnetic as expected for d^{10} systems.

XRD spectra. Figure 3 shows the XRD diffractograms for the complexes **A**, **B**, **C**, **D**, and **E**. Bragg's law was used to calculate the inter-planar spacing between the atoms (*d*-spacing; Å) [32]. The Scherrer equation was used to calculate the average particle size (*D*; nm) [33, 34]. The d-spacing and particle size for each complex were calculated based on the Bragg's diffraction angle (θ) of the highest line detected in the complexes' XRD diffractograms (2θ = 14.43°, 5.88°, 5.73°, 7.29°, and 16.77° for **A**, **B**, **C**, **D**, and **E**). The synthesized complexes were nanoscale-sized with *D* values of ~30, 23, 7, 31, and 20 nm for **A**, **B**, **C**, **D**, and **E**, respectively. Complex **C** had the smallest particle size; this was approximately one-quarter of the particle size of complexes **A** and **D**.

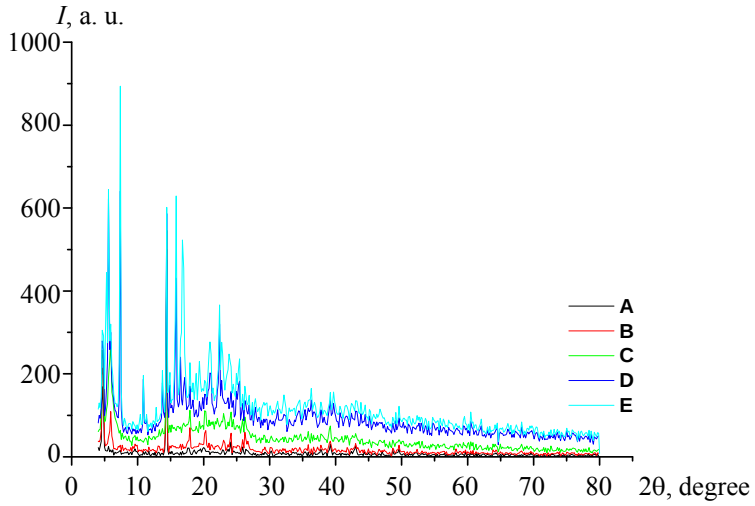

Fig. 3. XRD spectra of complexes **A, B, C, D,** and **E**.

Antimicrobial activity. The inhibition zones and screening results created by the synthesized complexes against the investigated microbes are shown in Fig. 4. The bacterial species were two Gram-negative strains (*E. coli* and *P. aeruginosa*) and two Gram-positive strains (*S. aureus* and *B. subtilis*) where the fungal species were *A. flavus* and *C. albicans*. The antibiotic drug tetracycline was used to compare the antibacterial results of HL and its complexes. Zones of inhibition (in mm/mg) were observed for tetracycline and were 32, 34, 30, and 34 mm/mg against *E. coli*, *P. aeruginosa*, *S. aureus,* and *B. subtilis*, respectively. The antibiotic drug amphotericin B was used to compare the antifungal results of HL and its complexes. Zones of inhibition (in mm/mg) were observed for amphotericin B and were 18 and 19 mm/mg against *A. flavus* and *C. albicans*, respectively. HL was found to exhibit antimicrobial activity against all tested microbes with different potency except for the *A. flavus* strain. The inhibition values for HL were 16, 20, 19, 25, 0, and 17 mm/mg against *E. coli*, *P. aeruginosa*, *S. aureus*, *B. subtilis*, *A. flavus,* and *C. albicans,* respectively. This antibacterial profile indicated that HL had moderate inhibitory activity against the investigated bacterial species except *B. subtilis*. HL showed good inhibitory activity against this strain. HL had no inhibitory activity against the fungal species *A. flavus*.

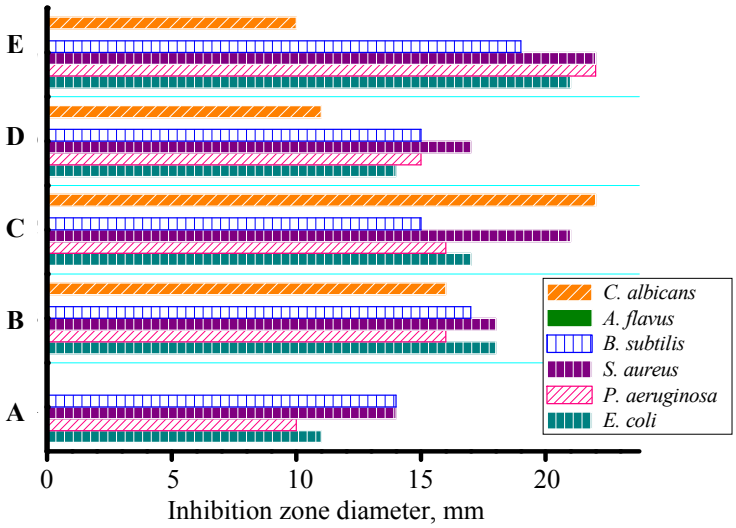

Fig. 4. The screening results for antimicrobial assay of the synthesized complexes towards the investigated microbes.

A. flavus remained resistant to the effects of the generated complexes after HL complexed with the metal ions. HL showed strong inhibitory activity against the other fungal species *C. albicans*. HL inhibited the growth of *C. albicans* with a zone of inhibition of 17 mm/mg, which was equal to 89% of the activity of amphotericin B. After the HL complex with Ni(II) ions, its potency against *Candida albicans* exceed that of the antifungal drug and reached to 22 mm/mg. Generally, the complexation of HL with the metal ions did not significantly change its antibacterial activity. The antibacterial activity of HL is more active against *B. subtilis* and *P. aeruginosa*. Complex **E** had the most potent antibacterial profile. The inhibition values for this complex were 21, 22, 22, and 19 mm/mg against *E. coli*, *P. aeruginosa*, *S. aureus*, and *B. subtilis*, respectively.

Conclusions. The plant growth regulator as 1-naphthylacetic acid was coordinated with five metal ions Mn(II), Co(II), Ni(II), Cu(II), and Zn(II) with a 1:2 metal-to-ligand molar ratio to form **A**, **B**, **C**, **D**, and **E** complexes, respectively. These complexes were structurally characterized using several microanalytical and spectroscopic techniques such as IR, ^{1}HNMR, UV-Vis, thermogravimetry, magnetic moment, and elemental analyses. The assignments of these analyses supported the suggested formulae of these complexes as $[MnL_2(H_2O)_2]$, $[CoL_2(H_2O)_2]$, $[NiL_2]$, $[CuL_2(H_2O)_2]$, and $[ZnL_2]H_2O$. In these complexes, two molecules of deprotonated HL ligand were coordinated to the metal ion as a bidentate carboxylate group. The Mn(II), Co(II), and Cu(II) ions had a six-coordinated environment whereas the Ni(II) and Zn(II) ions had four. The XRD techniques revealed that complex **C** had the smallest particle size (7 nm) versus the other synthesized complexes. The synthesized complexes were screened *in vitro* against six microbes using the Kirby-Bauer disc diffusion method: Gram-negative strains (*E. coli* and *P. aeruginosa*), Gram-positive strains (*S. aureus* and *B. subtilis*), and fungal species (*A. flavus* and *C. albicans*). Only complex **C** showed highly antifungal efficiency against *C. albicans* with a potency exceeding that of the antifungal positive control (amphotericin B) as well as HL itself.

Acknowledgements. This research was funded by the deanship of scientific Research at Princess Nourah bint Abdulrahman University through the Fast–track Research Funding program.

REFERENCES

1. N. Li, J. Chen, Y. Shi, *J. Chromatogr. A*, **1441**, 24–33 (2016).
2. G. Li, S. Lu, H. Wu, G. Chen, S. Liu, X. Kong, W. Kong, J. You, *J. Sep. Sci.*, **38**, No. 2, 187–196 (2015).
3. L. Wang, M. Wang, H. Yan, Y. Yuan, J. Tian, *J. Chromatogr. A*, **1368**, 37–43 (2014).
4. A. Gómez-Cadenas, J. Mehouachi, F. R. Tadeo, E. Primo-Millo, M. Talon, *Planta*, **210**, No. 4, 636–643 (2000).
5. Z. Wang, J. Xia, Q. Han, H. Shi, X. Guo, H. Wang, M. Ding, *Chin. Chem. Lett*., **24**, No. 7, 588–592 (2013).
6. J. A. Murillo Pulgarín, L. F. García Bermejo, I. Sánchez-Ferrer Robles, S. Becedas Rodríguez, *Phytochem. Anal*., **23**, No. 3, 214–221 (2012).
7. W. Guan, P. Xu, K. Wang, Y. Song, H. Zhang, *Food Chem. Toxicol*., **49**, 2869–2874 (2011).
8. A. Segura Carretero, C. Cruces Blanco, F. Alés Barrero, A. Fernández Gutiérrez, *J. Agric. Food Chem*., **46**, No. 2, 561–565 (1998).
9. R. L. Rardin, W. B. Tolman, S. J. Lippard, *New J. Chem*., **15**, 417 (1991).
10. I. G. Eremenko, S. E. Nefedov, A. A. Sidorov, *Inorg. Chem*., **38**, 3764 (1999).
11. L. G. Zhu, S. Kitagawa, H. Miyasaka, H. C. Chang, *Inorg. Chim. Acta*, **355**, 121 (2003).
12. K. Burger, J. Illes, B. Gyurcsik, *Carbohydr. Res*., **332**, 197 (2001).
13. Y. Chen, W. Cai, *Spectrochim. Acta A*, **62**, 863–868 (2005).
14. R. H. Holm, P. Kennepohl, E. I. Solomon, *Chem. Rev*., **96**, No. 7, 2239–2314 (1996).
15. A. W. Bauer, W. M. Kirby, C. Sherris, M. Turck, *Am. J. Clin. Pathol*., **45**, 493–496 (1966).
16. J. J. Biemer, *Ann. Clin. Lab. Sci*., **3**, 135–140 (1973).
17. M. C. Serrano, M. Ramírez, D. Morilla, A. Valverde, M. Chávez, A. Espinel-Ingroff, R. Claro, A. Fernández, C. Almeida, E. Martín-Mazuelos, *J. Antimicrob. Chemo-ther*., **53**, 739–742 (2004).
18. D. N. Sathyanarayana, *Vibrational Spectroscopy - Theory and Applications*, 2nd ed., New Age International (P) Ltd. Publishers, New Delhi (2004).
19. G. Socrates, *Infrared and Raman Characteristic Group Frequencies - Tables and Charts*, 3rd ed., Wiley, New York (2001).
20. V. Krishnakumar, R. Mathammal, S. Muthunatesan, *Spectrochim. Acta A*, **70**, No. 1, 210–216 (2008).

21. D. Lin-Vein, N. B. Colthup, W. G. Fateley, J. G. Grasselli, *The Handbook of Infrared and Raman Characteristic Frequencies of Organic Molecules*, Academic Press, San Diego (1991).
22. G. B. Deacon, R. J. Phillips, *Coord. Chem. Rev*., **33**, No. 3, 227–250 (1980).
23. P. B. Nagabalasubramanian, M. Karabacak, S. Periandy, *Spectrochim. Acta A*, **82**, 169–180 (2011).
24. K. Nakamoto, *Infrared Spectra of Inorganic and Coordination Compounds*, Wiley Interscience, John Wiley&Sons, New York, NY, USA (1970).
25. R. Jantas, B. Delczyk-Olejniczak, *Fibres Text. East. Eur.*, **13**, No. 1, 60–63 (2005).
26. J. R. Allan, N. D. Baird, A. L. Kassyk, *J. Therm. Anal*., **16**, No. 1, 79–90 (1979).
27. S. Sivakolunthu, S. Sivasubramanian, *J. Indian Chem. Soc*., **74**, 566–567 (1997).
28. A. B. P. Lever, *Coord. Chem. Rev*., **3**, No. 2, 119–140 (1968).
29. A. B. P. Lever, *Inorganic Electronic Spectroscopy*, 2nd ed., Elsevier, Amsterdam (1997).
30. F. A. Cotton, G. Wilkinson, C. A. Murillo, M. Bochmann, *Advanced Inorganic Chemistry*, 6th ed., Wiley, New York (1999).
31. S. Chandra, K. B. Pandeya, *Trans. Metal Chem*., **6**, No. 2, 110–113 (1981).
32. B. D. Cullity, S. R. Stock, *Elements of X-Ray Diffraction*, 3rd ed., Pearson Education Ltd., England (2014).
33. H. P. Klug, L. E. Alexander, *X-Ray Diffraction Procedures for Polycrystalline and Amorphous Materials*, New York, Wiley (1974).
34. M. A. Estermann, W. I. F. David, In: *Structure Determination from Powder Diffraction Data (SDPD)*, Eds. W. I. F. David, K. Shankland, I. B. Mccusker, Ch. Baerlocher, Oxford Science Publications, New York (2002).